Nativelike Structure and Stability in a Truncation Mutant of a Protein Minidomain: The Peripheral Subunit-Binding Domain†

Shari Spector,‡ Paul Young,§ and Daniel P. Raleigh*,‖

Department of Physiology and Biophysics, State University of New York at Stony Brook, Stony Brook, New York 11794-8661, Department of Chemistry, York College, City University of New York, Jamaica, New York 11451, Department of Chemistry, State University of New York at Stony Brook, Stony Brook, New York 11794-3400, and Graduate Programs in Biophysics and in Molecular and Cellular Biology, State University of New York at Stony Brook, Stony Brook, New York 11794

Received December 10, 1998; Revised Manuscript Received January 28, 1999

ABSTRACT: Despite its small size, the peripheral subunit-binding domain from the dihydrolipoamide acetyltransferase component of the *Bacillus stearothermophilus* pyruvate dehydrogenase multienzyme complex adopts a unique, compact structure. To determine whether the full 43 residue sequence is required for the domain to adopt a stable, nativelike structure, 3 proteins of different lengths were prepared. Psbd41 corresponds to residues 3−43 of the domain, psbd36 spans residues 6−41, and psbd33 comprises residues 7−39. Psbd41 folds in a cooperative, two-state fashion with a T_m of 53 °C and a stability at 25 °C of 2.2 kcal mol^{-1}. Psbd36 is nearly as stable with a T_m of 48 °C and a stability of 1.8 kcal mol^{-1}. Similar *m*-values and heat capacities suggest that psbd36 and psbd41 bury approximately the same surface area. Minimal differences in $C_\alpha H$ and NH chemical shifts between psbd41 and psbd36 show that the two sequences adopt the same tertiary fold. On a per residue basis, $\Delta H°$ and $\Delta C°_p$ fall within the range typical for single-domain globular proteins. Psbd33 is significantly less stable. It is not fully folded at 25 °C, and at all temperatures it shows broadened NMR lines. ANS titrations provide evidence that this is due to an equilibrium between nativelike and unfolded molecules rather than formation of a molten globule. The fraction of psbd33 molecules which are folded appear to adopt the same structure as the full-length domain. Thus, although more than the 33 residue core is required to form a fully stable native structure, the entire sequence is not required for folding.

Small, stably folded proteins have become popular model systems for experimental, computational, and theoretical studies of protein folding, and are attractive targets for de novo protein design. In addition to being very amenable to experimental studies, they also are ideal for theoretical studies because there are fewer interactions to model. Theoretical arguments based upon thermodynamic considerations have suggested that sequences shorter than 50 amino acids would not be able to adopt a stable, compact fold in the absence of additional stabilizing interactions (*1*). However, there are now a few examples of small proteins that fold in the absence of disulfide cross-links and without binding metals or other ligands (*2*−*6*).

There is also considerable interest in the minimization of protein structures. The minimization of ligands is one area of active interest. For example, recent work by Wells and co-workers has led to the minimization of protein A (*7*). Minimized proteins should also prove useful as well-defined structural scaffolds for the presentation of peptide libraries (*8*, *9*). Furthermore, miniproteins are more suitable for synthetic chemistry approaches and offer the prospect of preparing in high yield variant proteins that incorporate unnatural amino acids.

The peripheral subunit-binding domain serves as a good starting point for such studies. This domain from the dihydrolipoamide acetyltransferase component of the pyruvate dehydrogenase multienzyme complex in *Bacillus stearothermophilus* was originally isolated by limited proteolysis (*10*, *11*). Its short 43 amino acid sequence comprises 2 parallel α-helices connected by a loop containing a short stretch of 3_{10}-helix (Figure 1). This structure lacks disulfide bridges and does not bind metal ions or other ligands. The structure is stabilized by an interesting hydrogen bonding network involving the buried, charged side chain of Asp34 in the second helix and the backbone amides of Gly23, Thr24, Gly25, and Leu31 in the loop. There is an additional hydrogen bond from Asp34 to the side chain hydroxyl group of Thr24 (*2*). In addition to adopting a compact fold, the

† This work was supported by NIH Grant R29GM544233 to D.P.R. P.Y. was supported by a MARC Faculty Senior Fellowship from the NIH (1F33GM1862001). The NMR facility at SUNY Stony Brook is supported by a grant from the NSF (CHE9413510). The Spex Fluorolog fluorometer was purchased using funds from the NSF (CHE9709164). D.P.R. is a Pew Scholar in the Biomedical Sciences. S.S. was supported in part by a Graduate Council Fellowship from the Office of Graduate Studies at the State University of New York at Stony Brook.

* Corresponding author. E-mail: draleigh@ccmail.sunysb.edu.

‡ Department of Physiology and Biophysics, State University of New York at Stony Brook.

§ Department of Chemistry, City University of New York.

‖ Department of Chemistry and Graduate Programs in Biophysics and in Molecular and Cellular Biology, State University of New York at Stony Brook.

10.1021/bi982915k CCC: $18.00 © 1999 American Chemical Society
Published on Web 03/11/1999

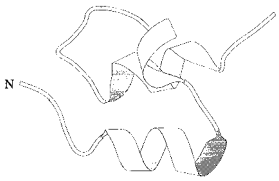

1 11
VIAMPSVRKY AREKGVDIRL

21 31
VQGTGKNGRV LKEDIDAFLA

41
GGA

FIGURE 1: Molscript diagram (*39*) and sequence of the peripheral subunit-binding domain. The figure was prepared using the NMR structure published by Kalia et al. (*2*), PBD code 2pdd. The best representative from the ensemble of NMR structures was determined using the program NMRCLUST (*33*).

structure undergoes cooperative unfolding transitions (*6*) unlike many small, isolated domains.

The structured core of the peripheral subunit-binding domain as determined by NMR[1] encompasses 33 residues, ranging from Val7 at the start of the first α-helix through Leu39 at the end of the second α-helix (*2*). In addition, the region from Met4 to Ser6 appears to adopt a set of right-handed helical conformations. The three N-terminal and four C-terminal residues appear to be largely disordered. To determine whether these apparently disordered residues are necessary for the peripheral subunit-binding domain to adopt a stable, native fold, we have prepared 2 truncation mutants and compared them to a 41 residue protein that we have previously described. This protein, designated psbd41, comprises Ala3−Gly43 (*6*). All residue numbers correspond to the positions in the full-length peripheral subunit-binding domain. The first truncation mutant, psbd36, is 36 residues long and spans from Ser6 to Gly41. Ser6 is located immediately before the start of the first α-helix and was included because it can potentially form a favorable N-capping interaction (*12*). At the carboxyl end, Ala40 was included because it is favorable for alanine to adopt a helical conformation, and Gly41 was included because it can stabilize a helix via a C-capping interaction (*12*). The other truncation mutant, psbd33, is 33 residues long and includes only those residues assigned to the structured core. Here, we present the results of a detailed thermodynamic analysis of the unfolding transitions of these proteins, including a more extensive characterization of the thermodynamics of psbd41 than we reported previously. We also show that although more than the 33 residue core is required for the formation of a stable, nativelike structure, the entire sequence is not required for full nativelike stability and cooperative folding. This work represents the first detailed thermodynamic characterization of a cooperatively folded structure that is smaller than 50 residues.

MATERIALS AND METHODS

Materials. PAL-PEG-PS resin was purchased from Perseptive Biosystems (Framingham, MA). TBTU and HBTU were purchased from Advanced Chemtech (Louisville, KY). Fmoc-protected amino acids were purchased from both of these companies. ANS was purchased from Molecular Probes (Eugene, OR). All other solvents and reagents were obtained from Fisher Scientific (Springfield, NJ).

Peptide Synthesis and Purification. Psbd41 was prepared and purified as described previously (*6*). In this work, two additional peptides were prepared and purified using the same conditions. Psbd36 spans residues Ser6−Gly41, and psbd33 is Val7−Leu39. All of the peptides have acetylated N-termini and amidated C-termini. All purification was by reverse-phase high-performance liquid chromatography (HPLC) with a C18 preparative column (Vydac). Unfortunately, the purification scheme that worked well for psbd41 left psbd36 and psbd33 with a significant remaining impurity, and an additional HPLC step was required. The first two steps for psbd36 and psbd33 were the same as for psbd41. The third HPLC purification step consisted of a water/acetonitrile gradient containing 0.06% (v/v) HCl. All of the peptides were greater than 95% pure. The identity of the peptides was confirmed by matrix-assisted laser desorption and ionization time-of-flight mass spectrometry (MALDI-TOF). Psbd41 had an experimental molecular mass of 4430.5 Da (expected molecular mass 4429.2 Da). The experimental molecular mass of psbd36 was 3997.1 Da (expected molecular mass 4001.6 Da). Psbd33 had a measured molecular mass of 3787.0 Da (expected molecular mass 3786.4 Da).

Circular Dichroism. All CD experiments described in this paper were performed on an Aviv 62A DS circular dichroism spectrophotometer in a buffer containing 2 mM phosphate, 2 mM borate, 2 mM citrate, 50 mM NaCl, pH 8.0. Far-UV CD spectra are the average of five repeats in a 0.1 mm cuvette. Near-UV CD spectra are the average of 10 repeats in a 1 cm cuvette. The peptide concentrations for all experiments were determined by UV spectroscopy, measuring the absorbance at 276 nm in 6 M GdnHCl, 20 mM NaH_2PO_4, pH 6.5, using an extinction coefficient of 1450 M^{-1} cm^{-1} (*13*). In addition, to check for aggregation the concentration dependence of the CD signal was monitored for psbd33. The mean residue ellipticity was shown to be independent of concentration.

ANS Titrations. ANS was dissolved in methanol, and its concentration was measured using an extinction coefficient of 6800 M^{-1} cm^{-1} at 370 nm (*14*). ANS titrations were performed as described previously (*6*) and monitored using a Spex Fluorolog spectrophotometer. ANS binding by psbd36 was monitored at 25 °C by titrating with a stock solution of 793 μM psbd36 to give a protein concentration range of 0−65.5 μM psbd36. The titration with an 841 μM stock solution of psbd33 was performed at 6 °C over a final concentration range of 0−103.2 μM psbd33. An ANS titration of psbd41 was described previously (*6*).

NMR Spectroscopy. All spectra were acquired on a Varian Instruments Inova 500 MHz nuclear magnetic resonance

[1] Abbreviations: ANS, 1-anilinonaphthalene-8-sulfonate; CD, circular dichroism; DQF-COSY, double quantum filtered correlation spectroscopy; Fmoc, N^{α}-9-fluorenylmethyloxycarbonyl; GdnHCl, guanidine hydrochloride; HBTU, 2-(1*H*-benzotriazol-1-yl)-1,1,3,3-tetramethyluronium hexafluorophosphate; HPLC, high-performance liquid chromatography; MALDI-TOF, matrix-assisted laser desorption and ionization time-of-flight mass spectrometry; NMR, nuclear magnetic resonance; NOE, nuclear Overhauser effect; NOESY, nuclear Overhauser effect spectroscopy; PAL-PEG-PS, poly(ethylene glycol) polystyrene Fmoc support for peptide amides; TBTU, 2-(1*H*-benzotriazol-1-yl)-1,1,3,3-tetramethyluronium tetrafluoroborate; T_m, midpoint of thermal denaturation transition; TOCSY, total correlation spectroscopy; UV, ultraviolet; ΔASA, change in accessible surface area.

spectrometer using standard presaturation for water suppression. The peptides were dissolved in 90% H_2O/10% D_2O, pH 5.1, with (tetramethylsilyl)propionate as a chemical shift standard. One-dimensional NMR spectra were acquired at 10 or 25 °C using standard presaturation methods. In addition, several two-dimensional homonuclear spectra were acquired at 10 °C to aid in the resonance assignments of psbd36 and to determine whether assignments of psbd33 would be feasible. The NMR samples were 4 mM in psbd36 or 1.4 mM in psbd33. All 2D spectra were acquired using time proportional phase incrementation (*15*) for quadrature detection. DQF-COSY (double quantum filtered correlated spectroscopy) spectra were acquired for both proteins with a matrix size of 1024 × 8192. TOCSY (total correlated spectroscopy) and NOESY (nuclear Overhauser effect spectroscopy) spectra were obtained for psbd36. These matrixes were 512 × 2048. Two TOCSY spectra were acquired with mixing times of 75 and 30 ms, and the NOESY spectrum with a mixing time of 250 ms.

Thermal Denaturations. Thermal denaturations were monitored by far-UV CD (222 nm) and near-UV CD (280 nm) in a stirred 1 cm cuvette. The temperature was raised from 2 to 90 °C by 2 °C intervals. A 1.2 °C overshoot for 10 s allowed the sample to equilibrate faster at each new temperature. The sample was allowed to equilibrate for 1.2 min, and the signal was averaged for 45 s. Reversibility was ascertained by comparing the ellipticity at 2 °C after a thermal denaturation to the initial ellipticity at 2 °C. Thermal denaturations of psbd41 were greater than 98% reversible, those of psbd36 were greater than 93% reversible, and for psbd33 they were greater than 92% reversible. All thermal denaturations were analyzed by nonlinear least-squares curve-fitting using SigmaPlot (Jandel Scientific) and the equations reported by Tan et al. (*16*) after correction for the typographical error of a factor of RT. Data are normalized to fraction unfolded.

Global Analysis of Three-Dimensional Denaturation Surfaces. Global analyses of thermal denaturations at a variety of concentrations of chemical denaturant were performed using guanidine hydrochloride as the denaturant for 9.4 μM psbd41, 12.1 μM psbd36, and 8.0 μM psbd33 and with urea for 10.8 μM psbd41, 12.4 μM psbd36, and 16.2 μM psbd33. For each sample, guanidine and urea concentrations were determined by measuring the change in refractive index (*17*). The reversibility of each of the thermal denaturations was determined as described above and varied with denaturant concentration. Reversibility ranged from 88 to 100% for psbd41 and psbd36 denatured by urea and from 80 to 98% for these two proteins denatured by guanidine. Reversibility was lower for psbd33, ranging from 74 to 95% in urea and from 78 to 93% in guanidine.

The data were then analyzed using a modified Gibbs−Helmholtz equation which includes an additional term for the denaturant dependence of the free energy of denaturation (*18*). The dependence of the free energy on denaturant concentration is modeled by

$$\Delta G^\circ_D(T,[\text{denaturant}]) = \Delta G^\circ_D(T) + m[\text{denaturant}] \quad (1)$$

The dependence of the free energy on temperature is given by the Gibbs−Helmholtz equation:

$$\Delta G^\circ_D(T) = \Delta H^\circ(T_m)\left(1 - \frac{T}{T_m}\right) - \Delta C^\circ_p\left[T_m - T + T\ln\left(\frac{T}{T_m}\right)\right] \quad (2)$$

These equations are combined with the standard expression that describes the sigmoidal unfolding transition. The dependence of the slopes of the pre- and post-transition planes on the temperature and the denaturant concentration is described by the parameters a_n, b_n, c_n and a_d, b_d, and c_d. The CD signal as a function of temperature and denaturant is then given by

$$\Theta(T,[\text{denaturant}]) = \{(a_n + b_nT + c_n[\text{denaturant}]) + (a_d + b_dT + c_d[\text{denaturant}])e^{-(\Delta G^\circ_D(T,[\text{denaturant}])/RT)}\}/\{1 + e^{-(\Delta G^\circ_D(T,[\text{denaturant}])/RT)}\} \quad (3)$$

There are 10 adjustable parameters in the analysis: T_m, $\Delta H^\circ(T_m)$, m, and ΔC°_p, and the 6 parameters that describe the base planes. The Gibbs−Helmholtz equation may also be rearranged to fit for ΔG°_D, ΔH°, and ΔS° at any temperature.

Isothermal Chemical Denaturation. Guanidine hydrochloride denaturations were monitored by far-UV CD at 222 nm in a stirred 1 cm cuvette. Denaturations of a 17.1 μM sample of psbd41 and a 16.2 μM sample of psbd36 were performed at 25 °C. Since psbd33 is not fully folded at 25 °C, the denaturation of 15.5 μM psbd33 was performed at 4 °C. All guanidine denaturations were performed by diluting a concentrated stock solution of peptide into either buffer or 8 M GdnHCl. The aliquot of the stock was dispensed with a Hamilton syringe into a volumetric flask. This ensures that the peptide concentration is the same in both solutions. The solution of peptide in buffer was titrated to approximately 4 M GdnHCl using the solution of peptide in 8 M GdnHCl. The other half of the curve was obtained by titrating a sample in 8 M GdnHCl with peptide in pure buffer. The final GdnHCl concentration was chosen so that it is less than that of the final point in the low guanidine portion of the curve. GdnHCl concentration was measured for each data point based on the change in refractive index as described above. Guanidine denaturation is shown to be reversible because the unfolding and refolding curves meet. Data were analyzed by nonlinear least-squares curve-fitting using SigmaPlot (Jandel Scientific).

Error Analysis. The error in the parameters obtained by nonlinear regression was determined using the method described by Shoemaker et al. (*19*). Briefly, for each parameter the nonlinear regressions were repeated holding that parameter constant. The chi-squared value obtained was then compared to the value for the best fit using an *F*-test to determine the 95% confidence limits. In this manner, the upper and lower limits for each parameter were determined. The error in a parameter obtained from a nonlinear least-squares fit is not necessarily symmetric.

RESULTS

Truncation Mutants of the Peripheral Subunit-Binding Domain Are Monomeric. All of the proteins in this study remain monomeric over the concentration ranges used for these experiments. Using a combination of analytical ultra-

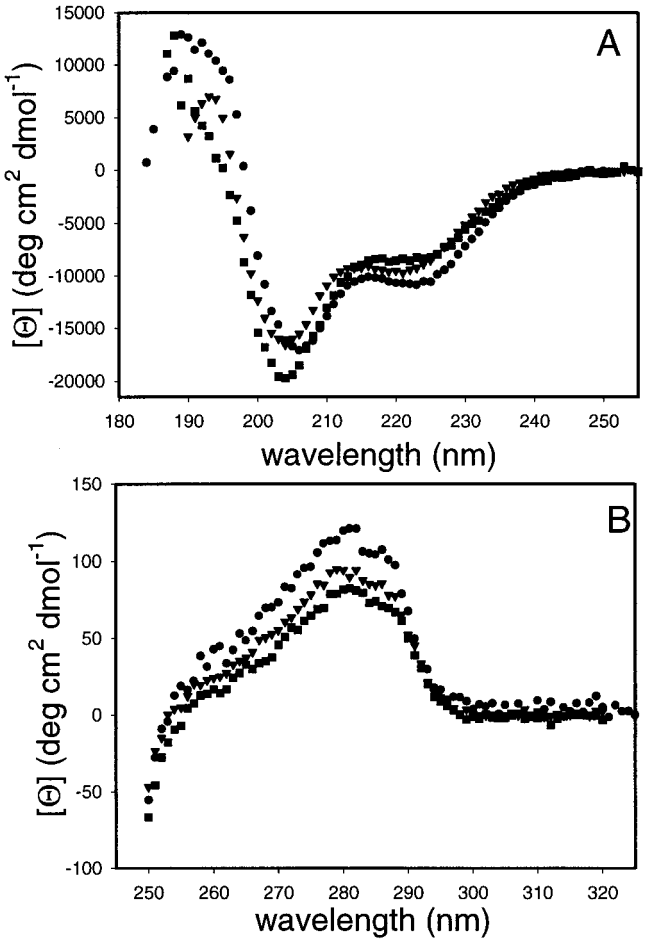

FIGURE 2: (A) Far-UV CD spectra of 403 μM psbd41 (circles), 272 μM psbd36 (triangles), and 338 μM psbd33 (squares). (B) Near-UV CD spectra of 379 μM psbd41 (circles), 272 μM psbd36 (triangles), and 338 μM psbd33 (squares). The spectra were recorded at pH 8.0, 25 °C.

centrifugation and concentration-dependent circular dichroism (CD), psbd41 has been previously shown to be monomeric at concentrations up to 3.05 mM (*6*). In addition, the midpoint of thermal denaturation for psbd41 is independent of concentration over the range studied, 9−435 μM. Psbd36 and psbd33 are also monomeric. For psbd36, the midpoint of thermal denaturation is independent of concentration over the studied range of 11−285 μM. One-dimensional proton NMR spectra are identical over the concentration range of 332 μM − 4 mM. Again for psbd33, the midpoint of thermal denaturation is independent of concentration from 8 to 338 μM. Also, the molar ellipticity at 222 nm is independent of concentration over the studied range of 10−703 μM. Finally, NMR spectra of a 467 μM sample and a 1.8 mM sample are identical. Thus, over the concentration range of at least 8 μM to 1.8 mM psbd33 appears to be monomeric.

Truncation Mutants of the Peripheral Subunit-Binding Domain Are Folded. Psbd41 has been previously shown to be folded and to adopt a structure that is nearly identical to the 43 residue peripheral subunit-binding domain studied by Kalia et al. (*2*), as evidenced by near- and far-UV CD and by NMR (*6*). Like psbd41, psbd36 and psbd33 appear to adopt a structure similar to the full-length peripheral subunit-binding domain. The far-UV CD spectrum of psbd36 is very similar in shape and intensity to psbd41 (Figure 2A). In addition, the maximum in the near-UV CD spectrum is only

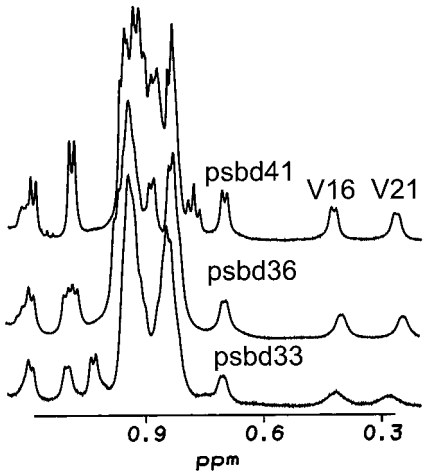

FIGURE 3: Methyl region of the proton NMR spectra of psbd41 (top), psbd36 (center), and psbd33 (bottom). The ring-current-shifted methyl resonances from Val16 and Val21 are labeled.

a little less intense (Figure 2B). CD spectra of psbd36 are identical at 25 and 4 °C. Based upon the intensities of the minima in the CD spectra at 222 nm and at 204 nm, psbd33 appears to be less helical at 25 °C than psbd41 or psbd36 (Figure 2A). Although psbd33 has a near-UV CD signal, the intensity of this band is also significantly decreased (Figure 2B) compared to the larger proteins. However, the rotational strengths of the helical bands and of the near-UV band increase at lower temperatures (data not shown; see thermal denaturations below), suggesting that psbd33 is not fully folded at 25 °C.

NMR provides additional evidence that psbd36 is folded and adopts a structure similar to the full-length domain. NMR studies also suggest that the fraction of psbd33 molecules that are folded adopt a structure similar to that of the full-length protein. The one-dimensional proton NMR spectra of both proteins show the characteristic ring-current-shifted methyl protons of Val16 and Val21 (Figure 3), although for psbd33 at room temperature they are significantly broadened and shift back downfield toward their unfolded chemical shifts. At low temperature (10 °C), they are shifted further upfield, with chemical shifts more like their counterparts in psbd41 and psbd36. These observations suggest that psbd33 is not completely folded at 25 °C. In contrast, the line widths and chemical shifts of these resonances in the NMR spectra of psbd41 and psbd36 are the same at 10 and 25 °C (data not shown). Another resonance that is resolved in the one-dimensional NMR spectrum and is very suggestive of nativelike structure is the downfield-shifted amide proton of Thr24 which is involved in a hydrogen bonding network to the buried, charged aspartate residue at position 34. In the wild-type protein, this amide appears at 10.01 ppm. It is at 9.98 ppm for psbd41, 9.94 ppm for psbd36, and 9.60 ppm for psbd33. The amide protons of Gly23 and Gly25 participate in the hydrogen bonding network involving Asp34, and as a consequence their amide protons are also shifted significantly downfield. In psbd41, the Gly23 amide proton has a chemical shift of 8.71 ppm, and the Gly25 amide proton is at 8.85 ppm. In psbd36, these resonances appear at 8.65 and 8.81 ppm, respectively. Since they are not resolved in the one-dimensional NMR spectrum, their chemical shifts for psbd33 could not be determined.

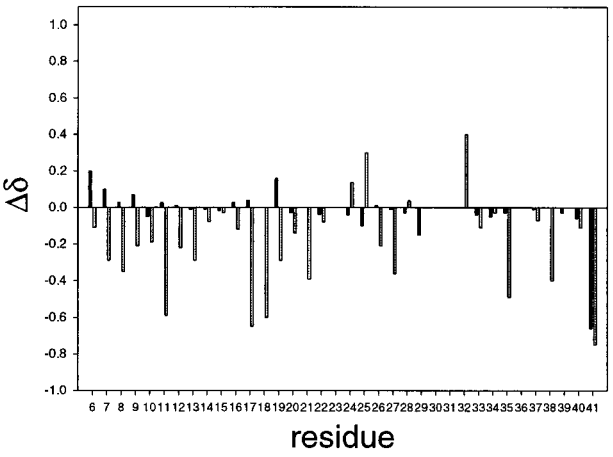

FIGURE 4: Comparison of psbd36 CαH chemical shifts to the full-length domain and to random coil values. Chemical shift differences, $\Delta\delta$, are reported with the wild-type (*2*) or random coil values (*20*) subtracted from the psbd36 values. Black bars: CαH (psbd36 minus wild type). Gray bars: CαH (psbd36 minus random coil). The absence of a bar means that the chemical shift deviation is less than 0.01 ppm. Values were not determined for residues 23, 30, 31, or 36.

Nearly complete backbone assignments were obtained for psbd36 using a combination of TOCSY, NOESY, and DQF-COSY experiments. Comparison of the chemical shifts observed at 10 °C, pH 5.1, for the 36mer to those obtained by Kalia et al. at 20 °C, pH 5.0 (*2*), suggests that psbd36 adopts essentially the same structure as the full-length peripheral subunit-binding domain. Some of the chemical shift differences between psbd36 and the assignments obtained by Kalia for the intact peripheral subunit-binding domain may arise from the slight differences in conditions under which the NMR spectra were acquired. Also, differences near the termini are most likely due to the removal of residues. Of the 34 amide resonances that could be assigned, 20 differed in chemical shift by 0.1 ppm or less, and 11 were different by 0.11−0.20 ppm. Of the remaining two, one was near the amino terminus where several residues have been removed. Similarly, of the 32 $C_\alpha H$ resonances that were assigned, 28 had chemical shift differences of 0.1 ppm or less and 3 were between 0.11 and 0.20 ppm different. The only residue with a $C_\alpha H$ chemical shift that differed from Kalia's assignments by more than 0.2 ppm was the C-terminal residue. Such small differences would be highly unlikely if the structures of psbd41 and psbd36 were significantly different. In contrast, the $C_\alpha H$ chemical shift differences between psbd36 and those expected for a random coil (*20*) are much larger than between psbd36 and the full-length peripheral subunit-binding domain. These differences range from −0.75 to 0.40 ppm (Figure 4).

Although several of the resonances characteristic of the folded structure are evident in the one-dimensional spectrum of psbd33, the linewidths are too broad for assignments to be obtained from the two-dimensional spectra. Such broad linewidths may arise from several sources. One possibility is that the protein has aggregated, or that it associates to form dimers or higher order oligomers. However, we have demonstrated that psbd33 is monomeric up to 1.8 mM (see above), and the NMR experiments were performed at 1.4 mM. Also, not all of the resonances are significantly broadened, as would be expected if aggregation were occurring. Rather, the broadening increases with the difference between folded and random coil chemical shifts. Such chemical shift dependence of the linewidth is consistent with broadening due to conformational flexibility. This can occur if the protein is inherently flexible and does not adopt a unique tertiary structure, as is often observed for molten globule states (*21*), or if the protein is folding and unfolding in the intermediate-exchange time regime (microseconds to milliseconds) (*22*).

To determine whether psbd33 is nativelike or molten globule-like, a titration with 1-anilinonaphthalene-8-sulfonate (ANS) was performed. This fluorescent dye is commonly used as a probe for molten globule formation (*23*). ANS seldom binds to the native state of proteins unless they have exposed hydrophobic patches on their surfaces, and it usually does not bind to the unfolded state. Even at a 13-fold excess of psbd33 to ANS, there was little increase in quantum yield and no change in emission maximum, indicating that psbd33 does not bind ANS (data not shown). One worry is that the proteins in this study are too small to have sufficient hydrophobic surface area to bind a molecule as large as ANS. However, while psbd33, psbd36 (data not shown), and psbd41 do not bind ANS (*6*), a mutant in which the buried, charged aspartic acid at position 34 has been replaced by asparagine has been shown to be molten globule-like and to bind ANS (*6*). Thus, since psbd33 is not a molten globule and does not aggregate, the NMR lines are likely broadened due to conformational exchange, most probably between a folded and unfolded form, on the intermediate-exchange time scale. This is consistent with the NMR spectra of psbd33, in which the broadening is proportional to the chemical shift difference between the folded and the unfolded state.

Thermal Denaturations. Thermal denaturations were performed to compare the thermal stability of each truncation mutant to that of psbd41. In contrast to many small, helical peptides, all three proteins show cooperative thermal denaturation curves as monitored by near- and far-UV circular dichroism (CD) (Figure 5A). Thermal denaturation is greater than 98% reversible for psbd41, 93% reversible for psbd36, and 92% reversible for psbd33. The data were analyzed using the Gibbs−Helmholtz equation to obtain the midpoint of the thermal denaturation, T_m, and the enthalpy, $\Delta H°(T_m)$. The $\Delta C°_p$ used in the analysis, 0.43 kcal mol^{-1} K^{-1}, comes from global analysis of thermal denaturations in the presence of guanidine or urea (see below). For each protein, the values of T_m and $\Delta H°(T_m)$ obtained by near- and far-UV CD are in good agreement, which is consistent with two-state folding. Furthermore, the value of T_m obtained is independent of the value of the heat capacity used in the analysis over the range of 0.30−0.65 kcal mol^{-1} K^{-1}, and the variation in $\Delta H°(T_m)$ caused by using different values of $\Delta C°_p$ in this range is less than the uncertainty in $\Delta H°(T_m)$. The cooperativity of the transition is clearly apparent from the raw data (Figure 5A, inset) as well as from the normalized data (Figure 5A). Psbd41 has a T_m of 53 °C and the enthalpy, $\Delta H°(T_m)$, is 31.7 kcal mol^{-1}. Using the Gibbs−Helmholtz equation, the calculated stability of psbd41 in water is 2.19 kcal mol^{-1} at 25 °C. The discrepancy between this value and that determined from guanidine denaturation of psbd41 and reported in a previous study (*6*) is due to ionic strength effects on protein stability, which are discussed in more detail below. Psbd36 is nearly as thermally stable with a T_m of 48 °C, and $\Delta H°(T_m)$ is 30.3 kcal mol^{-1}, corresponding to a stability in

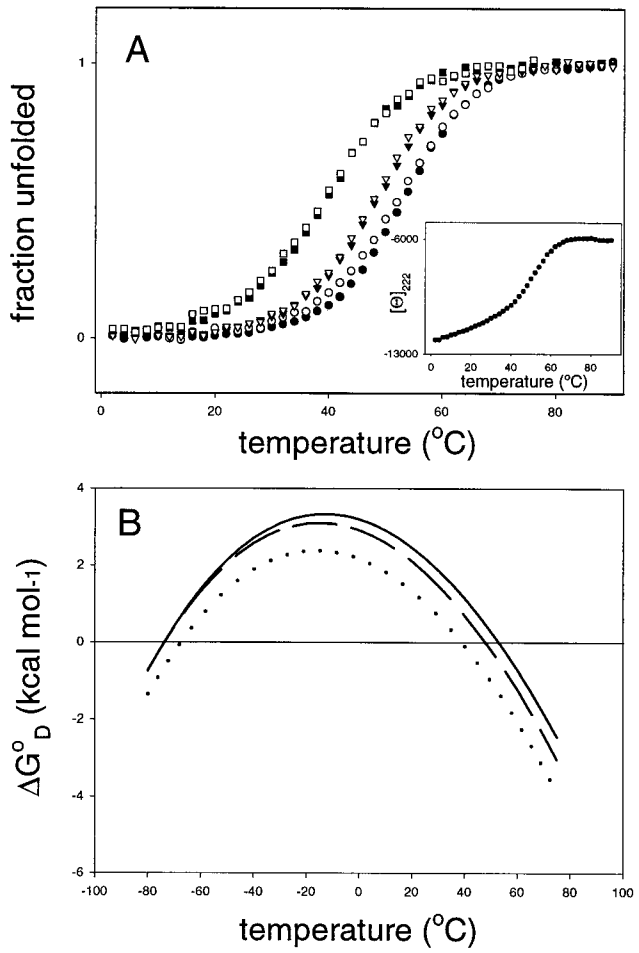

FIGURE 5: (A) Thermal denaturations of psbd41 (circles), psbd36 (triangles), and psbd33 (squares). Solid symbols represent the data from thermal denaturations monitored by far-UV CD at 222 nm, and open symbols correspond to thermal denaturations monitored by near-UV CD at 280 nm. Experiments were conducted at pH 8.0. The inset shows a sample data set for the thermal denaturation of psbd41 monitored by far-UV CD. (B) Gibbs−Helmholtz plots of the temperature dependence of the stability of the peripheral subunit-binding domain. The Gibbs−Helmholtz equation was solved using the values of $\Delta H°(T_m)$ and T_m obtained from the thermal denaturations and a $\Delta C°_p$ value of 0.43 kcal mol^{-1} K^{-1}. Solid line: psbd41. Dashed line: psbd36. Dotted line: psbd33.

water of 1.81 kcal mol^{-1} at 25 °C. The peptide corresponding to just the core, psbd33, is significantly less stable and is not fully folded at room temperature. Analysis of the data for psbd33 results in a T_m of only 39 °C. The enthalpy is also lower, 26.1 kcal mol^{-1}, and the stability in water is only 1.03 kcal mol^{-1} at 25 °C (Table 1). The value $\Delta G°_D$(25 °C) reported for psbd33 is an upper limit because in the analysis psbd33 is assumed to be 100% folded at low temperature, which does not appear to be true based on the NMR data.

Using the values of $\Delta H°(T_m)$ and T_m obtained from the thermal denaturations together with the $\Delta C°_p$ determined via global analysis, it is possible to prepare Gibbs−Helmholtz plots of the temperature dependence of the stability. Truncation results in a decrease in stability at all temperatures, rather than a significant change in the shape of the plot (Figure 5B). Psbd36 is more destabilized relative to psbd41 at high temperatures than at low temperatures. The plot for psbd33 is included for comparison, although because it is never fully folded the stability is overestimated at all temperatures. All three proteins have a temperature of maximum stability of approximately −10 °C. The predicted cold denaturation temperatures are very low, largely as a consequence of the small value of $\Delta C°_p$ observed for these proteins.

Global Free Energy Analysis and Determination of $\Delta C°_p$. It is possible to obtain a complete set of thermodynamic parameters for a protein folding transition by performing thermal denaturations at a variety of concentrations of chemical denaturant and doing a global analysis of the data using eqs 1−3 as described under Materials and Methods (*18*, *24*−*27*). From the analysis, one can obtain $\Delta C°_p$, $\Delta H°(T_m)$, T_m, and the *m*-value.

Global thermodynamic analyses were performed for psbd41, psbd36, and psbd33 both with guanidine hydrochloride (data not shown) and with urea as the chemical denaturant. Plots of the data obtained for psbd41 with urea are shown in Figure 6. The individual thermal denaturations within the data set show good cooperativity, although this is difficult to visualize in the surface plot. The analysis was complicated by several factors. The values of T_m obtained from the experiments with guanidine as the chemical denaturant were significantly higher than those obtained from a simple thermal denaturation. In contrast, the values of T_m obtained from experiments with urea as the chemical denaturant agree well with the values of T_m obtained from thermal denaturations. The stabilities at 25 °C, $\Delta G°_D$, determined from the global analysis using urea as the denaturant are also in better agreement with those obtained using the Gibbs−Helmholtz equation than with the stabilities determined from isothermal guanidine denaturations. The values of $\Delta C°_p$ determined using either guanidine or urea as the denaturant are in good agreement, differing by less than 10% for psbd36 and by less than 5% for psbd41.

The discrepancies in T_m and $\Delta G°_D$ between the techniques appear to result from the effect of ionic strength on the stability of the protein. Increasing the sodium chloride concentration increases the T_m of psbd41 in a nonlinear fashion, and thus it is probably the increased ionic strength in the presence of guanidine hydrochloride that affects the apparent stability of the protein. An apparent increase in the stability of a protein, as determined by guanidine denaturation compared to urea denaturation, has been observed for a number of proteins including apomyoglobin and cytochrome *c* (*28*), ribonuclease A (*29*), and several other proteins and peptides (*30*, *31*). The phenomenon has been shown to result from ionic strength effects (*28*, *31*).

The second complication with these experiments arises from the large uncertainties associated with the parameters determined from the curve fitting. The peripheral subunit-binding domain is a remarkably small protein, and, therefore, the values of its thermodynamic parameters are also quite small. Consequently, the values are difficult to determine precisely. In addition, because the data are being fit to equations with 10 adjustable parameters, small changes in any given parameter are easily compensated, thus further increasing the uncertainty. Since the *m*-value and $\Delta G°_D$ agree between the global analysis with guanidine and the isothermal guanidine denaturations, and the $\Delta H°(T_m)$ and T_m agree between the global analyses with urea and the thermal denaturations, the thermodynamic parameters obtained from the global analysis seem reasonable despite the uncertainties. Nevertheless, the only parameter from the global analysis that we have chosen to use is the value of $\Delta C°_p$.

Table 1: Thermodynamic Parameters for the Peripheral Subunit-Binding Domain and Its Truncation Mutants

protein	$\Delta H°(T_m)$[a]	T_m[a]	$\Delta G°_D$(25 °C)[b]	$\Delta C°_p$[c]	*m*-value urea[d]	*m*-value GdnHCl[e]
psb41	31.7 ± 1.7[f]	53 ± 0.4	2.19	0.43 ± 0.25	0.34 ± 0.11	0.67 ± 0.08
psbd36	30.3 ± 4.3	48 ± 1.2	1.81	0.44 ± 0.19	0.32 ± 0.07	0.64 ± 0.06
psbd33	26.1 ± 7.7	39 ± 3.6	1.03	0.44 ± 0.28	0.41 ± 0.10	0.50 ± 0.16

[a] Parameters obtained from thermal denaturations. $\Delta H°(T_m)$ in kcal mol^{-1}; T_m is in °C. [b] $\Delta G°_D$(25 °C) was obtained from the thermal denaturations using the Gibbs−Helmholtz equation and is reported in units of kcal mol^{-1}. [c] Heat capacities were obtained from the global analysis of thermal denaturations at various urea concentrations and are reported in units of kcal mol^{-1} K^{-1}. [d] The *m*-values obtained from global analysis with urea are reported in units of kcal mol^{-1} M^{-1}. [e] The *m*-values obtained from isothermal guanidine denaturations are reported in units of kcal mol^{-1} M^{-1}. The parameters for psbd41 and psbd36 were obtained at 25 °C and those for psbd33 at 4 °C. [f] Errors were obtained as described under Materials and Methods. Since errors are asymmetric, the larger deviation is reported.

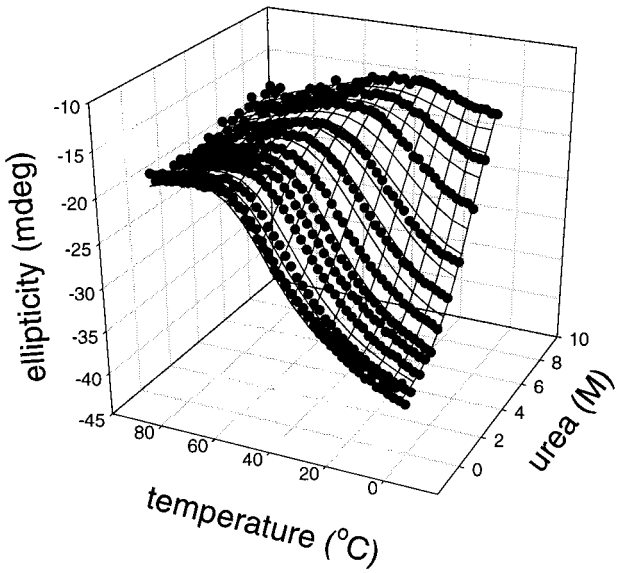

FIGURE 6: Global free energy analysis. The three-dimensional plot shows the dependence of the far-UV CD signal of psbd41 on temperature and urea concentration. Experiments were performed at pH 8.0.

The value of $\Delta C°_p$ is related to the change in accessible surface area upon folding (*32*). This relationship enables us to predict the expected value of $\Delta C°_p$. Using the best representative from the family of NMR structures (*33*) and the ACCESS routine from the software package WHATIF (*34*), it is possible to determine the difference in accessible surface area, ΔASA, between the folded and the unfolded protein. Furthermore, ΔASA can be broken down into contributions from polar and nonpolar surfaces. Based on these numbers, psbd41 is expected to have a $\Delta C°_p$ between 330 and 412 cal mol^{-1} K^{-1}. Since the residues removed from psbd41 to create psbd36 and psbd33 are thought to be largely unstructured and do not contribute to the hydrophobic core, the truncation mutants should have the same or a very similar heat capacity compared to the full-length domain.

The values of $\Delta C°_p$ obtained from the global analysis with urea are 430 cal mol^{-1} K^{-1} for psbd41 and 440 cal mol^{-1} K^{-1} for psbd36 (Table 1). The uncertainty in the heat capacity determined from global analysis is large, as is that for all of the thermodynamic parameters. However, these numbers are consistent with the predicted value. The agreement between the values of $\Delta C°_p$ determined for psbd41 and psbd36 is also reassuring. In addition, $\Delta C°_p$ obtained from global analysis with guanidine as the denaturant also agrees well with the urea data, with values of 450 cal mol^{-1} K^{-1} for psbd41 and 410 cal mol^{-1} K^{-1} for psbd36 (data not shown). Furthermore, it is important to point out that this is the only technique available for accurate determination of the heat capacity of these proteins. Because the value of $\Delta C°_p$ is so small, it cannot be measured accurately with microcalorimetry. The other commonly used technique to determine the heat capacity is to measure $\Delta H°(T_m)$ when the T_m is perturbed by changing the pH. However, the pH does not significantly alter the T_m, so it is not possible to obtain an accurate measure of the heat capacity using this approach.

Psbd33 is expected to have a heat capacity value very similar to those obtained for psbd41 and psbd36. The heat capacity determined for psbd33 with urea was in good agreement with those for psbd36 and psbd41 (440 cal mol^{-1} K^{-1}). Psbd33 is not fully folded at even the lowest temperatures, and it may be coincidental that the apparent value of $\Delta C°_p$ determined from urea agrees so well with the values for psbbd41 and psbd36. Since the values of $\Delta C°_p$ for psbd41 and psbd36 obtained using both guanidine and urea as the denaturant are in good agreement, the averaged value of all four numbers, 430 cal mol^{-1} K^{-1}, was used in the analysis of the thermal denaturations described above, including those for psbd33.

Analysis of m-Values. Like heat capacity, the *m*-value also depends on the difference in accessible surface area between the native and denatured states of a protein (*32*). A comparison of *m*-values is therefore useful in comparing the structures of the three proteins. Urea is not as strong a denaturant as guanidine, and therefore urea unfolding transitions appear broader and less cooperative. As a result, it is difficult to measure the *m*-value or stability from an isothermal urea denaturation of the peripheral subunit-binding domain. However, the *m*-values for urea denaturations can be determined from global analysis. Based on the global analyses with urea, psbd41 has an *m*-value of 0.34 kcal mol^{-1} M^{-1}, psbd36 has an *m*-value of 0.32 kcal mol^{-1} M^{-1}, and psbd33 has an *m*-value of 0.41 kcal mol^{-1} M^{-1} (Table 1). The predicted *m*-value of urea denaturation for psbd41 based on contributions to the change in accessible surface from polar and nonpolar surfaces is 0.25 kcal mol^{-1} M^{-1} (*32*, *35*), which is somewhat smaller than the measured values. Small *m*-values result in urea denaturations that are very broad, making it difficult to fit them accurately, and the differences between the observed and predicted *m*-values are comparable in magnitude to the uncertainty in the measured *m*-values. Guanidine hydrochloride is a stronger denaturant than urea, and *m*-values for guanidine-induced unfolding can be determined directly from the isothermal guanidine denaturation curves.

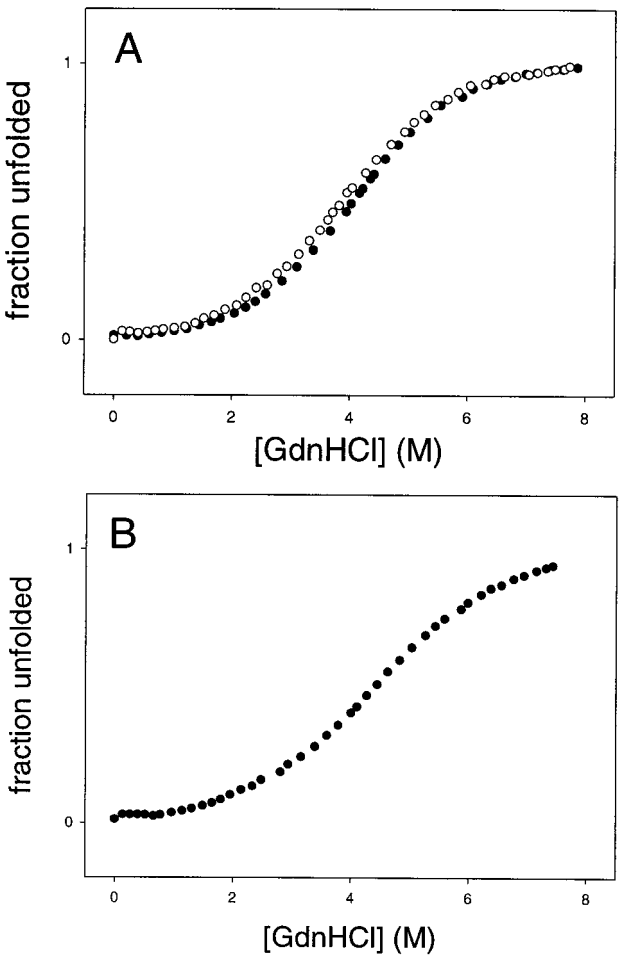

FIGURE 7: Guanidine denaturations. (A) Solid circles: psbd41, 25 °C. Open circles: psbd36, 25 °C. (B) Psbd33, 4 °C. All chemical denaturations were performed at pH 8.0.

When ionic strength affects the stability of a protein, as seen here, it may do so either through simple electrostatic interactions or via Hofmeister effects. Variations in ionic strength are expected to modulate the stability of the three proteins in approximately the same manner. The truncations made here should not alter the magnitude of any Hofmeister effects. Furthermore, chloride ion is neither kosmotropic nor chaotropic, and therefore is considered neutral within the Hofmeister series. Since none of the residues that have been removed in the truncation mutants is charged, electrostatic screening effects should also be essentially the same for each of these proteins. Thus, despite the effects of ionic strength on stability, it is reasonable for this set of proteins to compare the *m*-values determined from isothermal guanidine denaturations. Psbd41 has an *m*-value of 0.67 kcal mol^{-1} M^{-1} (Figure 7A). This value is slightly smaller than previously reported (*6*). The experiments described here have more data points and therefore provide a more accurate measure of the *m*-value. The *m*-value is also in good agreement with that predicted based on the change in accessible surface area. The predicted value, accounting for separate contributions from the polar and the nonpolar surface area, is 0.66 kcal mol^{-1} M^{-1} (*32*, *35*). Psbd36 has a comparable *m*-value of 0.64 kcal mol^{-1} M^{-1} (Figure 7A). Psbd33 is not fully folded at 25 °C, and therefore the guanidine denaturation of this truncation mutant was performed at 4 °C (Figure 7B). At this temperature, psbd33 has an *m*-value of 0.50 kcal mol^{-1} M^{-1}, but the error is on the order of ±0.16 kcal mol^{-1} M^{-1}. This is much larger than the errors observed for psbd41 and psbd36, which were ±0.08 and ±0.06 kcal mol^{-1} M^{-1}, respectively.

DISCUSSION

Although more than the 33 residues defined as the core are required for the peripheral subunit-binding domain to adopt a fully native structure at 25 °C, the full sequence is not required. Psbd33 is only partially folded, even at temperatures as low as 4 °C. Nonetheless, the available evidence suggests that the folded fraction of molecules appears to have the same structure as the longer proteins. It is particularly interesting that more than 33 residues are required for nativelike stability given that the NMR data obtained by Kalia et al. indicate that the residues missing from psbd33 are unstructured (*2*). Psbd36 not only adopts the same structure as psbd41 but also has comparable stability.

The peripheral subunit-binding domain is a very small protein, and, as expected, the values of its thermodynamic parameters are much smaller than are typically seen for globular proteins. However, the values are on the order expected for a protein of this size. As discussed above, the *m*-value for urea denaturation of psbd41, 0.34 kcal mol^{-1} M^{-1}, is a little larger than the predicted value of 0.25 kcal mol^{-1} M^{-1}, but this difference is similar in magnitude to the uncertainty in the parameter. The predicted *m*-value for guanidine denaturation is 0.66 kcal mol^{-1} M^{-1} based on the change in accessible surface area. This is in excellent agreement with the values obtained for psbd41 (0.67 kcal mol^{-1} M^{-1}) and psbd36 (0.64 kcal mol^{-1} M^{-1}). Similarly, the heat capacity determined for these proteins, 0.43 kcal mol^{-1} K^{-1}, is also in good agreement with the value calculated based on the change in accessible surface area (0.33−0.41 kcal mol^{-1} K^{-1}). On a per residue basis, this is at the low end (10.5 cal mol^{-1} K^{-1} for psbd41 and 11.8 cal mol^{-1} K^{-1} for psbd36) of what is commonly seen for globular proteins (10−18 cal mol^{-1} K^{-1}) (*36*−*38*) but is still within the normal range. The heat capacity difference between folded and unfolded proteins is commonly thought to be due to the hydrophobic effect. The observation that ΔC°_{p} is, on a per residue basis, within the range typically observed for globular proteins argues that the peripheral subunit-binding domain does not bury an exceptionally large amount of hydrophobic surface area on a per residue basis. Using the data obtained from the global analysis of thermal and urea denaturations, it is possible to calculate ΔH° at 25 °C. For psbd41, the enthalpy at 25 °C is 0.32 kcal mol^{-1} residue^{-1}, which is quite close to the average value of 0.40 kcal mol^{-1} residue^{-1} observed by Makhatadze and Privalov in their survey of 20 globular proteins. In the same study, they report an unfolding entropy per mole of residues between −0.5 and 2.0 kcal mol^{-1} K^{-1} with an average value of 0.5 kcal mol^{-1} K^{-1} (*38*). The values for psbd41 and psbd36 are 0.04 and 0.05 kcal mol^{-1} K^{-1}, respectively. Thus, although it is an extremely small protein, the peripheral subunit-binding domain appears to be a perfectly normal protein, gaining its stability from a normal balance between hydrophobic and nonhydrophobic interactions.

The peripheral subunit-binding domain is only marginally stable with a ΔG°_{D} of 2.2 kcal mol^{-1} at 25 °C in water and

3.1 kcal mol^{-1} at 4 °C. The domain, however, is part of a much larger protein and may be further stabilized by interactions with the rest of the molecule. It is interesting to note that the only other natural sequence of less than 50 residues which has been shown to fold cooperatively in the absence of disulfides is also part of a larger structure. The HP35 subdomain is a piece of the larger actin-bundling protein villin. This domain is also only marginally stable with a $\Delta G°_D$ determined by guanidine denaturation of 3.3 kcal mol^{-1} at 4 °C (*3*).

Small proteins make excellent targets for de novo design. However, the peripheral subunit-binding domain is only marginally stable, with a $\Delta G°_D$ of 2.2 kcal mol^{-1} at moderate salt concentrations (50 mM NaCl). Depending on the goal of the design experiment, this might be sufficient, given its reasonably high T_m of 53 °C. Psbd36, which is only slightly destabilized, should still make a reasonable starting point for such design studies. Furthermore, through mutagenesis it may be possible to evolve a variant of psbd36 that could adopt the same fold, but with greater stability.

NOTE ADDED IN PROOF

A crystal structure of the peripheral subunit-binding domain bound to the dihydrolipoamide dehydrogenase component of the pyruvate dehydrogenase multienzyme complex was recently solved (*40*). In the complex, helix 1 begins at Pro5, compared to Val7 in the solution structure (*6*). Helix 2 is also extended by one residue, including Ala40 instead of ending at Leu 39. This is consistent with our result that more than 33 residues are required for nativelike stability.

ACKNOWLEDGMENT

We thank Mr. Daniel Moriarty for collecting the MALDI-TOF mass spectra at the Center for the Analysis of the Structure of Biological Macromolecules at the State University of New York at Stony Brook. We also thank Dr. Brian Kuhlman for his assistance obtaining NMR data for psbd41.

REFERENCES

1. Privalov, P. L. (1992) in *Protein Folding* (Creighton, T. E., Ed.) pp 83−126, W. H. Freeman and Company, New York.
2. Kalia, Y. N., Brocklehurst, S. M., Hipps, D. S., Appella, E., Sakaguchi, K., and Perham, R. N. (1993) *J. Mol. Biol. 230*, 323−341.
3. McKnight, C. J., Doering, D. S., Matsudaira, P. T., and Kim, P. S. (1996) *J. Mol. Biol. 260*, 126−134.
4. McKnight, C. J., Matsudaira, P. T., and Kim, P. S. (1997) *Nat. Struct. Biol. 4*, 180−184.
5. Dahiyat, B. I., and Mayo, S. L. (1997) *Science 278*, 82−87.
6. Spector, S., Kuhlman, B., Fairman, R., Wong, E., Boice, J. A., and Raleigh, D. P. (1998) *J. Mol. Biol. 276*, 479−489.
7. Braisted, A. C., and Wells, J. A. (1996) *Proc. Natl. Acad. Sci. U.S.A. 93*, 5688−5692.
8. DeGrado, W. F., and Sosnick, T. R. (1996) *Proc. Natl. Acad. Sci. U.S.A. 93*, 5680−5681.
9. Mer, G., Kellenberger, E., and Lefevre, J.-F. (1998) *J. Mol. Biol. 281*, 235−240.
10. Duckworth, H. W., Jaenicke, R., Perham, R. N., Wilkie, A. O. M., Finch, J. T., and Roberts, G. C. K. (1982) *Eur. J. Biochem. 124*, 63−89.
11. Packman, L. C., Borges, A., and Perham, R. N. (1988) *Biochem. J. 252*, 79−86.
12. Richardson, J. S., and Richardson, D. C. (1988) *Science 240*, 1648−1652.
13. Gill, S. C., and von Hippel, P. H. (1989) *Anal. Biochem 182*, 319−326.
14. Cocco, M. J., and Lecomte, J. T. J. (1994) *Protein Sci. 3*, 267−281.
15. Marion, D., and Wütrich, K. (1983) *Biochem. Biophys. Res. Commun. 113*, 967−974.
16. Tan, Y.-J., Oliveberg, M., Davis, B., and Fersht, A. R. (1995) *J. Mol. Biol. 254*, 980−992.
17. Pace, C. N., Shirley, B. A., and Thomson, J. A. (1990) in *Protein Structure: A Practical Approach* (Creighton, T. E., Ed.) pp 311−330, Oxford University Press, Oxford, England.
18. Huang, G. S., and Oas, T. G. (1996) *Biochemistry 35*, 6173−6180.
19. Shoemaker, D. P., Garland, C. W., and Nibler, J. W. (1989) *Experiments in Physical Chemistry*, 5th ed., McGraw-Hill Publishing Company, New York.
20. Wishart, D. S., Bigam, C. G., Holm, A., Hodges, R. S., and Sykes, B. D. (1995) *J. Biomol. NMR 5*, 67−81.
21. Baum, J., Dobson, C. M., Evans, P. A., and Hanley, C. (1989) *Biochemistry 28*, 7−13.
22. Huang, G. S., and Oas, T. G. (1995) *Proc. Natl. Acad. Sci. U.S.A. 92*, 6878−6882.
23. Seminostov, G. V., Rodionova, N. A., Razgulyaev, O. I., Uversky, V. N., Gripas, A. F., and Gilmanshin, R. I. (1991) *Biopolymers 31*, 119−128.
24. McCrary, B. S., Edmondson, S. P., and Shriver, J. W. (1996) *J. Mol. Biol. 264*, 784−805.
25. Nicholson, E. M., and Scholtz, J. M. (1996) *Biochemistry 35*, 11369−11378.
26. Yi, Q., Scalley, M. L., Simons, K. T., Gladwin, S. T., and Baker, D. (1997) *Fold. Des. 2*, 271−280.
27. Kuhlman, B., and Raleigh, D. P. (1998) *Protein Sci. 7*, 2405−2412.
28. Hagihara, Y., Aimoto, S., Fink, A. L., and Goto, Y. (1993) *J. Mol. Biol. 231*, 180−184.
29. Yao, M., and Bolen, D. W. (1995) *Biochemistry 34*, 3771−3781.
30. Pace, C. N. (1975) *CRC Crit. Rev. Biochem. 3*, 1−43.
31. Smith, J. S., and Scholtz, J. M. (1996) *Biochemistry 35*, 7292−7297.
32. Myers, J. K., Pace, C. N., and Scholtz, J. M. (1995) *Protein Sci. 4*, 2138−2148.
33. Kelley, L. A., Gardner, S. P., and Sutcliffe, M. J. (1996) *Protein Eng. 9*, 1063−1065.
34. Vriend, G. (1990) *J. Mol. Graph. 8*, 52−56.
35. Spolar, R. S., Livingstone, J. R., and Record, M. T., Jr. (1992) *Biochemistry 31*, 3947−3955.
36. Privalov, P. L., and Gill, S. J. (1988) *Adv. Protein Chem. 39*, 191−234.
37. Knapp, S., Mattson, P. T., Christova, P., Berndt, K. D., Karshikoff, A., Vihinen, M., Smith, C. I. E., and Ladenstein, R. (1998) *Proteins: Struct., Funct., Genet. 31*, 309−319.
38. Makhatadze, G. I., and Privalov, P. L. (1995) *Adv. Protein Chem. 47*, 307−425.
39. Kraulis, P. J. (1991) *J. Appl. Crystallogr. 24*, 946−950.
40. Mande, S. S., Sarfaty, S., Allen, M. D., Perham, R. N., and Hol, W. G. J. (1996) *Structure 4*, 277−286.

BI982915K